

# Receding Horizon Control Based Online Motion Planning with Partially Infeasible LTL Specifications

Mingyu Cai<sup>1</sup>, Hao Peng<sup>2</sup>, Zhijun Li<sup>3</sup>, Hongbo Gao<sup>3</sup>, and Zhen Kan<sup>3</sup>

**Abstract**—This work considers online optimal motion planning of an autonomous agent subject to linear temporal logic (LTL) constraints. The environment is dynamic in the sense of containing mobile obstacles and time-varying areas of interest (i.e., time-varying reward and workspace properties) to be visited by the agent. Since user-specified tasks may not be fully realized (i.e., partially infeasible), this work considers hard and soft LTL constraints, where hard constraints enforce safety requirements (e.g. avoid obstacles) while soft constraints represent tasks that can be relaxed to not strictly follow user specifications. The motion planning of the agent is to generate policies, in decreasing order of priority, to 1) guarantee the satisfaction of safety constraints; 2) mostly satisfy fulfill constraints (i.e., minimize the violation cost if desired tasks are partially infeasible); and 3) optimize the objective of rewards collection (i.e., visiting dynamic areas of more interests). To achieve these objectives, a relaxed product automaton, which allows the agent to not strictly follow the desired LTL constraints, is constructed. A utility function is developed to quantify the differences between the revised and the desired motion plan, and the accumulated rewards are designed to bias the motion plan towards those areas of more interests. Receding horizon control is synthesized with an LTL formula to maximize the accumulated utilities over a finite horizon, while ensuring that safety constraints are fully satisfied and soft constraints are mostly satisfied. Simulation and experiment results are provided to demonstrate the effectiveness of the developed motion strategy.

**Index Terms**—Formal Method, Model Predictive Control, Multi-Objective Optimization, Graph Theory

## I. INTRODUCTION

Motion planning of autonomous agents has broad potential applications ranging from driverless cars navigating urban environments subject to complex traffic rules [1] to autonomous vehicles (e.g., an unmanned ground or aerial vehicle) performing search and rescue missions in uncertain environments after a natural disaster [2], and to robotic systems dynamically cooperating with human operators in manufacturing and medical care [3]–[6]. While there is a growing demand for these applications, autonomous agents so far have not been fully used. One major challenge is that desired missions are often composed of multiple tasks subject to complex specifications (e.g., complex traffic rules or sophisticated human-robot interactions), which classical motion planning approaches, such as the point-to-point navigation [7], the traveling salesman

problem [8], and the orienteering problem [9], are no longer capable of. Another major challenge is that the operating environment is often complex, e.g., dynamic and not fully known *a priori*. The user-specified missions can be partially infeasible if the real environment is found during the runtime to be prohibitive to the agent. Therefore, a particular motivation for this work is to consider online optimal motion planning of an autonomous agent that can handle complex missions and environments.

### A. Related Work

Linear temporal logic (LTL) is a formal language capable of expressing rich task specifications and providing intuitive translation from human language to syntactically correct formulas. Due to its rich expressivity in describing complex missions, motion planning with LTL specifications has generated substantial interest (cf. [10]–[17] to name a few). For instance, in [18], co-safe linear temporal logic was used for a mobile robot to perform service tasks in an office environment. In [19], standard LTL tasks were employed for a noisy differential-drive vehicle to maximize the probability of completing user-specified tasks in an uncertain environment. In [20], task allocation and planning for temporal logic goals were developed for a heterogeneous multi-robot system. Other representative results on motion planning with LTL specifications include information-guided persistent monitoring [21], hybrid control of multi-agent systems with formation constraints [22], cooperative control of mobile robots with intermittent connectivity [13], and control synthesis over stochastic systems considering both feasible and infeasible tasks [15]–[17].

Despite considerable progress in the literature, new challenges arise when the operating environment is dynamic and uncertain. The environment may have time-varying events of interest and dynamic obstacles that are not fully known to the agent *a priori*, which requires the agent to dynamically adapt its motion plan to the changing environment. To address dynamic environments, model predictive control, also referred as receding horizon control (RHC), has been integrated with LTL specifications and successfully applied in various applications. For instance, the motion planning of a vehicle in an urban-like environment was considered in [23], where a provably correct control strategy that combines LTL specifications and RHC was developed. In [24], LTL-based receding horizon motion planning was developed for a finite-state deterministic system to maximize reward collection while

<sup>1</sup>Department of Mechanical Engineering, The University of Iowa, Iowa City, IA, 52246, USA.

<sup>2</sup>Apex.AI Inc, Palo Alto, CA, 94303, USA.

<sup>3</sup>Department of Automation, University of Science and Technology of China, Hefei, Anhui, China.

satisfying desired task specifications. Recently, LTL based RHC was extended to mobile robot networks for cooperative environmental monitoring [25]. Other results based on RHC with temporal logical specifications include [26]–[29]. The work [30] proposed a sampling-based planning algorithm that reactively and efficiently achieved global temporal logic goals and satisfied short-term dynamic requirements.

Approaches based on RHC have been proven as effective tools to handle dynamic environments in the aforementioned results. However, these results rely on a key assumption that the operating environment is feasible. That is, there exists a feasible motion plan in the dynamic environment that satisfies the desired LTL specifications. However, the assumption of a feasible dynamic environment can be restrictive, and, in practice, not all user-specified LTL task specifications can be realized by the agent. For instance, the agent can be tasked to visit a sequence of areas of interest, where some of them may not be reachable (e.g., surrounded by water that the ground robot cannot traverse) in the real environment. LTL constraints that cannot be fully satisfied are often relaxed to allow the tasks to be fulfilled as much as possible. In [31], a least-violating control strategy for finite LTL was developed to allow potentially infeasible tasks within a partially known workspace. In [32], sampling-based algorithm for minimum violation motion planning was developed. In [33] and [34], partial satisfaction of Co-safe LTL specifications was considered to deal with uncertain environment. These strategies were further extended in [18] for motion planning of service robots. In [35],  $LDL_f$  is applied with a graph search algorithm to treat the soft constraints. However, only finite horizon motion planning was considered in the works of [18] and [31]–[35]. When considering infinite horizon motion planning, the minimal revision problem was considered in [36] and [37] with the goal of making the revised motion planning close to the original LTL. In [38], minimum violation of graph-based algorithm is presented, which is further extended in [39] by considering shortest plans. In [12], cooperative control synthesis of multi-agent systems was considered in a partially known environment to maximize the satisfaction of the specified LTL constraints. However, [36]–[38] focus on the single objective of minimal revision to the original LTL. [12] and [39] optimize the static cost (shortest path) via graph-based method, without considering motion planning with respect to time-varying optimization objectives (e.g., reward collection). It is not yet understood how user-specific missions can be successfully managed to solve optimization problems with time-varying parameters under a dynamic environment, where desired tasks can be partially infeasible.

## B. Contributions

This work considers online motion planning of an autonomous agent subject to LTL mission constraints. The operating environment is assumed to be dynamic and only partially known to the agent. The environment also has time-varying areas of interest to be visited by the agent. The areas of interest are associated with time-varying rewards and time-varying state labels, where the rewards indicate

the relative importance and state labels indicate time-varying workspace properties. Since previously user-specified tasks may not be fully realized (i.e., partially infeasible) by the agent in the environment, this work considers hard and soft LTL constraints, where hard constraints enforce safety requirement (e.g. avoid obstacles) while soft constraints represents tasks that can be relaxed to not strictly follow user-specifications if the environment does not permit. The motion planning of the agent is to generate policies, in decreasing order of priority, to 1) formally guarantee the satisfaction of safety constraints; 2) mostly satisfy soft constraints (i.e., minimize the violation cost if desired tasks are partially infeasible); and 3) collect time-varying rewards as much as possible (i.e., visiting areas of more interests).

To achieve these objectives, the motion of the agent is modeled by a finite deterministic transition system (DTS), with a limited sensing capability of detecting obstacles and observing rewards within a local area. A relaxed product automaton is constructed based on the DTS and the non-deterministic Büchi automaton (NBA) generated from the desired LTL specifications, which allows the agent to not strictly follow the desired LTL constraints. A utility function composed of the violation cost and the accumulated rewards is developed, where the violation cost is designed to quantify the differences between the revised and the desired motion plan. The accumulated rewards are designed to bias the motion plan towards those areas of more interests. Since the workspace is only partially known, real-time sensed information is used to update the agent’s knowledge about the environment. Under the assumption of time-varying rewards that can only be locally observed, RHC is synthesized with an LTL formula to maximize the accumulated utilities over a finite horizon, while ensuring that safety constraints are fully satisfied and soft constraints are mostly satisfied.

Differing from most existing works that mainly focus on motion planning with feasible LTL constraints, this work considers control synthesis of an agent operating in a complex environment with dynamic properties and time-varying areas of interest that can only be observed locally, wherein user-specified tasks might not be fully feasible. Integrated with the RHC framework, a relaxed product automaton is developed to handle partially infeasible tasks by quantifying the violation of soft constraints. RHC is synthesized with an LTL formula to maximize the accumulated utilities over a finite horizon, while formally ensuring the objectives in decreasing orders: 1) hard constraints are fully satisfied; 2) soft constraints are mostly satisfied; 3) accumulate rewards that change dynamically are locally optimized at each time-step over finite horizon. This work is closely related to [24]. However, we extend the approach in [24] by considering partially infeasible tasks where the energy function is redesigned to take into account the violation cost of the revised path to the desired path. In addition, rigorous analysis is provided, showing the correctness of the produced infinite trajectory and the recursive feasibility of RHC-based motion planning. It’s also shown the computational complexity in automaton update is reduced. Simulation and experiment results are provided to demonstrate its effectiveness.

## II. PRELIMINARIES

An LTL formula is built on a set of atomic propositions  $\Pi$ , which are properties of system states that can be either true or false, standard Boolean operators such as  $\wedge$  (conjunction),  $\vee$  (disjunction),  $\neg$  (negation), and temporal operators such as  $\diamond$  (eventually),  $\bigcirc$  (next),  $\square$  (always), and  $\cup$  (until). A word satisfies  $\phi$  if  $\phi$  is true at the first position of the word;  $\square\phi$  means  $\phi$  is true for all future moments;  $\diamond\phi$  means  $\phi$  is true at some future moments;  $\bigcirc\phi$  means  $\phi$  is true at the next moment; and  $\phi_1\cup\phi_2$  means  $\phi_1$  is true until  $\phi_2$  becomes true. The semantics of an LTL formula are defined over words, which are an infinite sequence  $o = o_0o_1\dots$  with  $o_i \in 2^\Pi$  for all  $i \geq 0$ , where  $2^\Pi$  represents the power set of  $\Pi$ . Denote by  $o \models \phi$  if the word  $o$  satisfies the LTL formula  $\phi$ . More expressivity can be achieved by combining temporal and Boolean operators. Detailed descriptions of the syntax and semantics of LTL can be found in [40].

An LTL formula can be translated to a nondeterministic Büchi automaton (NBA).

**Definition 1.** An NBA is a tuple  $\mathcal{B} = (S, S_0, \Delta, \Sigma, \mathcal{F})$ , where  $S$  is a finite set of states;  $S_0 \subseteq S$  is the set of initial states;  $\Sigma \subseteq 2^\Pi$  is the input alphabet;  $\Delta: S \times \Sigma \rightarrow 2^S$  is the transition function; and  $\mathcal{F} \subseteq S$  is the set of accepting states.

Let  $s \xrightarrow{\sigma} s'$  denote the transition from  $s \in S$  to  $s' \in S$  under the input  $\sigma \in \Sigma$  if  $s' \in \Delta(s, \sigma)$ . Given a sequence of input  $\sigma = \sigma_0\sigma_1\sigma_2\dots$  over  $\Sigma$ , a run of  $\mathcal{B}$  generated by  $\sigma$  is an infinite sequence  $s = s_0s_1s_2\dots$  where  $s_0 \in S_0$ , and  $s_{i+1} \in \Delta(s_i, \sigma_i)$  for each  $i > 0$ . If the input  $\sigma$  can generate at least one run  $s$  that intersects the accepting states  $\mathcal{F}$  infinitely many times,  $\mathcal{B}$  is said to accept  $\sigma$ . For any LTL formula  $\phi$  over  $\Pi$ , one can construct an NBA with input alphabet  $\Sigma = 2^\Pi$  accepting all and only words that satisfy  $\phi$  [40]. Let  $\mathcal{B}_\phi$  denote the NBA generated from the LTL formula  $\phi$ . To convert an LTL formula to an NBA, readers are referred to [41] for algorithms and implementations.

A dynamical system with finite states evolving deterministically under control inputs can be modeled by a weighted finite deterministic transition system (DTS) [42].

**Definition 2.** A weighted finite DTS is a tuple  $\mathcal{T} = (Q, q_0, \delta, \Pi, L, \omega)$ , where  $Q$  is a finite set of states;  $q_0 \in Q$  is the initial state;  $\delta \subseteq Q \times Q$  is the state transitions;  $\Pi$  is the finite set of atomic propositions;  $L: Q \rightarrow 2^\Pi$  is the labeling function; and  $\omega: \delta \rightarrow \mathbb{R}^+$  is the weight function.

Let  $q \rightarrow q'$  denote the state transition  $(q, q') \in \delta$  in  $\mathcal{T}$ , where  $q, q' \in Q$ . Each transition in  $\delta$  is associated with a weight determined by  $\omega$ . A path of  $\mathcal{T}$  is an infinite sequence  $\mathbf{q} = q_0q_1\dots$  where  $q_i \in Q$  and  $(q_i, q_{i+1}) \in \delta$  for  $i \geq 0$ . A path  $\mathbf{q}$  over  $\mathcal{T}$  generates an output sequence  $\sigma = \sigma_0\sigma_1\dots$  where  $\sigma_i = L(q_i)$  for  $i \geq 0$ . The transition  $(q, q') \in \delta$  is deterministic, which implies a one-to-one map between  $\mathbf{q} = q_0q_1\dots$  and the transitions  $(q_0, q_1), (q_1, q_2), \dots$ , thus resulting in a DTS.

Let  $R_k(q)$  denote the varying reward associated with a state  $q$  at time-step  $k$ . Given a trajectory at this time  $\mathbf{q}_k = q_0q_1\dots q_n$ , the accumulated reward along the trajectory  $\bar{s}_k^{\mathcal{P}}$

is  $\mathbf{R}_k(\mathbf{q}) = \sum_{i=1}^N R_k(q_i)$ . The time-varying reward function represents the event of interest in the environment<sup>1</sup>. The optimization of rewards at each time-step is one of objectives in this paper.

Model checking a DTS against a LTL formula is based on the construction of the product automaton between the DTS and the corresponding NBA. Given the defined NBA and DTS, a weighted product automaton can be constructed as follows.

**Definition 3 (Weighted Product Automaton).** Given a weighted DTS  $\mathcal{T} = \{Q, q_0, \delta, \Pi, L, \omega\}$  and an NBA  $\mathcal{B} = (S, S_0, \Delta, \Sigma, \mathcal{F})$ , the product automaton  $\tilde{\mathcal{P}} = \mathcal{T} \times \mathcal{B}$  is defined as a tuple  $\tilde{\mathcal{P}} = \{P_{\tilde{\mathcal{P}}}, P_{\tilde{\mathcal{P}}0}, L_{\tilde{\mathcal{P}}}, \Delta_{\tilde{\mathcal{P}}}, \mathcal{F}_{\tilde{\mathcal{P}}}, \omega_{\tilde{\mathcal{P}}}\}$ ,

- $P_{\tilde{\mathcal{P}}} = Q \times S$  is the set of states, e.g.,  $p_{\tilde{\mathcal{P}}} = (q, s)$  and  $p'_{\tilde{\mathcal{P}}} = (q', s')$  where  $p_{\tilde{\mathcal{P}}}, p'_{\tilde{\mathcal{P}}} \in P_{\tilde{\mathcal{P}}}$ ;
- $P_{\tilde{\mathcal{P}}0} = \{q_0\} \times S_0$  is the set of initial states;
- $L_{\tilde{\mathcal{P}}}: P_{\tilde{\mathcal{P}}} \rightarrow 2^\Pi$  is a labeling function, i.e.,  $L_{\tilde{\mathcal{P}}}(p_{\tilde{\mathcal{P}}}) = L(q)$ ;
- $\Delta_{\tilde{\mathcal{P}}} \subseteq P_{\tilde{\mathcal{P}}} \times P_{\tilde{\mathcal{P}}}$  is the set of transitions, i.e.,  $((q, s), (q', s')) \in \Delta_{\tilde{\mathcal{P}}}$  if and only if  $q \rightarrow q'$  and  $s \xrightarrow{L(q)} s'$ ;
- $\mathcal{F}_{\tilde{\mathcal{P}}} = Q \times \mathcal{F}$  is the set of accepting states;
- $\omega_{\tilde{\mathcal{P}}}: \Delta_{\tilde{\mathcal{P}}} \rightarrow \mathbb{R}^+$  is the weight function, i.e.,  $\omega_{\tilde{\mathcal{P}}}(p_{\tilde{\mathcal{P}}}, p'_{\tilde{\mathcal{P}}}) = \omega(q, q')$ .

Let  $(q, s) \rightarrow_{\tilde{\mathcal{P}}} (q', s')$  denote the transitions from  $(q, s) = s_{\tilde{\mathcal{P}}}$  to  $(q', s') = p'_{\tilde{\mathcal{P}}}$  in  $\tilde{\mathcal{P}}$  if  $(p_{\tilde{\mathcal{P}}}, p'_{\tilde{\mathcal{P}}}) \in \Delta_{\tilde{\mathcal{P}}}$ . A trajectory  $\mathbf{p}_{\tilde{\mathcal{P}}} = (q_0, s_0)(q_1, s_1)\dots$  of  $\tilde{\mathcal{P}}$  is an infinite sequence where  $(q_0, s_0) \in S_{\tilde{\mathcal{P}}0}$  and  $(q_i, s_i) \rightarrow_{\tilde{\mathcal{P}}} (q_{i+1}, s_{i+1})$  for all  $i \geq 0$ . The trajectory  $\mathbf{p}_{\tilde{\mathcal{P}}}$  is called accepting if and only if  $s_{\tilde{\mathcal{P}}}$  intersects  $\mathcal{F}_{\tilde{\mathcal{P}}}$  infinitely many times. Let  $\gamma_{\mathcal{T}}(\mathbf{p}_{\tilde{\mathcal{P}}}) = q_0q_1\dots$  denote the projection of  $\mathbf{p}_{\tilde{\mathcal{P}}}$  on the transition system  $\mathcal{T}$ . Note that a trajectory  $s_{\tilde{\mathcal{P}}}$  can be uniquely projected onto  $\mathcal{T}$  by  $\gamma_{\mathcal{T}}$ . By the construction of  $\tilde{\mathcal{P}}$  from  $\mathcal{T}$  and  $\mathcal{B}$ ,  $s_{\tilde{\mathcal{P}}}$  is an accepting trajectory on  $\tilde{\mathcal{P}}$  if and only if  $\gamma_{\mathcal{T}}(\mathbf{p}_{\tilde{\mathcal{P}}})$  satisfies the LTL formula corresponding to  $\mathcal{B}$ .

## III. EXAMPLE AND PROBLEM FORMULATION

### A. Example Demonstration

As a running example, consider a robot operating in an environment abstracted to a labeled grid-like graph  $\mathcal{G} = (\mathcal{V}, \mathcal{E}, \Pi)$ , where the node set  $\mathcal{V}$  represents the partitioned areas, the edge set  $\mathcal{E}$  indicates possible transitions, and the atomic propositions  $\Pi = \{\text{Base}, \text{Supply}, \text{Report}, \text{Obstacle}, \text{Survey}\}$  indicate the labeled properties of the areas<sup>2</sup>, as shown in Fig. 1. The robot motion in the environment is then represented by the finite DTS  $\mathcal{T}$  in Def. 2 evolving over  $\mathcal{G}$ , where  $Q$  represents the node set  $\mathcal{V}$ , and the possible transitions  $\delta$  are captured by the edge set  $\mathcal{E}$ . As an example application, a specific surveillance mission  $\phi$  is considered in this work, where the robot is required to visit a set of stations repetitively,

<sup>1</sup>Local sensing rewards are considered in this work. Other types of rewards, such as in trajectory optimization [43], information gathering [44], and local tasks [26], are also applicable.

<sup>2</sup>Abstracted environments have been widely used in the literature, and many existing partition methods, such as triangulation and rectangular grids, can be applied to partition the workspace [45].

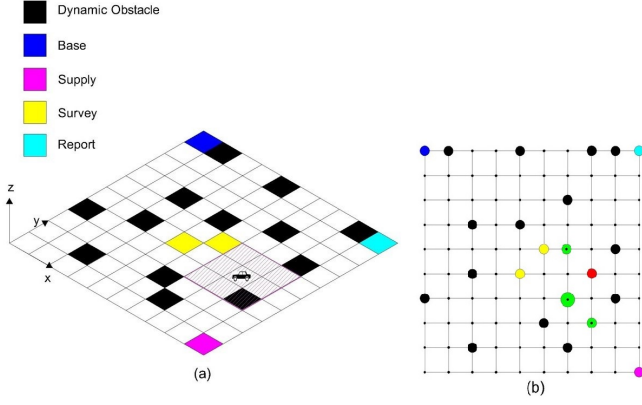


Figure 1: (a) Example of a partitioned operating environment, where the shaded area around the vehicle indicates its local sensing. (b) The corresponding abstracted grid-like graph of (a), where the size of green dots is proportional to their reward values and the red dot represents the vehicle.

while maximizing the collected rewards and avoiding obstacles on the way to the destinations. Due to the consideration of partially infeasible environment, the user-specified LTL task  $\phi$  consists of hard constraints  $\phi_h$  and soft constraints  $\phi_s$ , i.e.,  $\phi = \phi_h \wedge \phi_s$ , where  $\phi_h$  models the constraint of collision avoidance that have to be fully satisfied while  $\phi_s$  models soft constraints that can be relaxed if it's infeasible in current environment. In this case, The desired task of the robot within the environment  $\mathcal{G}$  is described by an LTL formula  $\phi$  over the atomic propositions  $\Pi$ . A variety of tasks can be represented in LTL formulas, such as the sequential visit of Survey and Report (i.e.,  $\diamond(\text{Survey} \wedge \diamond\text{Report})$ ), the persistent surveillance of visiting Base infinitely many times (i.e.,  $\square\diamond\text{Base}$ ), and avoiding collision while achieving a task  $\phi$  (i.e.,  $\square(\neg\text{Obstacle} \wedge \phi)$ ). More expressivity of tasks can be achieved based on the combination of temporal and Boolean operators over  $\Pi$ . The environment is assumed to be only partially known to the robot, i.e., the robot may know the static destinations to visit but not the obstacles it may encounter during mission operation. The environment is dynamic in the sense of containing real-time dynamic obstacles and time-varying rewards associated with each state. The time-varying reward  $R_k(q) \in \mathbb{R}^+$  is given at each step. It is further assumed that the robot can only detect obstacles, observe rewards, and sense node labels within a local area around itself. As an example application, the robot is required to complete the given LTL task, while maximizing the collected rewards. More detailed task descriptions can be found in Section VI-A.

The description above is just an representation and this work can be extended in several directions. The LTL tasks can be defined for other sets of atomic propositions and requirements and the rewards-optimization problem can be easily applied to other meaningful time-varying objectives.

### B. Problem formulation

Given the time-varying reward function  $R_k(q_i)$ ,  $\forall i = 1, \dots, N$  associated with each states in DTS that is unknown

a priori, and is only observed and optimised locally online at time  $k$ , the motion planning problem in this work is presented as follows.

**Problem 1.** Given a deterministic transition system  $\mathcal{T}$ , and a user-specified LTL formula  $\phi = \phi_h \wedge \phi_s$ , the control objective is to design an online planning strategy, in decreasing order of priority, that 1)  $\phi_h$  is fully satisfied; 2)  $\phi_s$  is fulfilled as much as possible if the task is not feasible; and 3) rewards collection at each time-step is maximized over a finite horizon during mission operation.

In Problem 1, by saying to fulfill  $\phi_s$  as much as possible, we mean to minimize the violation of  $\phi_s$ , which will be formally defined in Section IV-A.

## IV. RELAXED AUTOMATON AND PROBLEM FORMULATION

Sec. IV-A discusses how  $\phi_s$  can be relaxed to allow motion revision and how the violation of  $\phi_s$  can be quantified. Sec. IV-B describes the construction of an energy function that enforces the satisfaction of accepting conditions. Sec. IV-C presents how local sensing can be used to update the robot's knowledge about the environment to facilitate motion revision.

### A. Relaxed LTL Specifications

Let  $\mathcal{B}_h = (S_h, S_{h0}, \Delta_h, \Sigma_h, \mathcal{F}_h)$  and  $\mathcal{B}_s = (S_s, S_{s0}, \Delta_s, \Sigma_s, \mathcal{F}_s)$  denote the NBA corresponding to  $\phi_h$  and  $\phi_s$ , respectively. The relaxed product automaton for  $\phi = \phi_h \wedge \phi_s$  is constructed as follows.

**Definition 4 (Relaxed Product Automaton).** Given a weighted DTS  $\mathcal{T} = \{Q, q_0, \delta, \Pi, L, \omega\}$  and the NBA  $\mathcal{B}_h$  and  $\mathcal{B}_s$ , the relaxed product automaton  $\mathcal{P} = \mathcal{T} \times \mathcal{B}_h \times \mathcal{B}_s$  is defined as a tuple  $\mathcal{P} = \{S_{\mathcal{P}}, S_{\mathcal{P}0}, L_{\mathcal{P}}, \Delta_{\mathcal{P}}, \mathcal{F}_{\mathcal{P}}, \omega_{\mathcal{P}}, h_{\mathcal{P}}, v_{\mathcal{P}}\}$ , where

- $S_{\mathcal{P}} = Q \times S_h \times S_s$  is the set of states, e.g.,  $s_{\mathcal{P}} = (q, s_h, s_s)$  and  $s'_{\mathcal{P}} = (q', s'_h, s'_s)$  where  $s_{\mathcal{P}}, s'_{\mathcal{P}} \in S_{\mathcal{P}}$ ;
- $S_{\mathcal{P}0} = \{q_0\} \times S_{h0} \times S_{s0}$  is the set of initial states;
- $L_{\mathcal{P}} : S_{\mathcal{P}} \rightarrow 2^{\Pi}$  is a labeling function, i.e.,  $L_{\mathcal{P}}(s_{\mathcal{P}}) = L(q)$ ;
- $\Delta_{\mathcal{P}} \subseteq S_{\mathcal{P}} \times S_{\mathcal{P}}$  is the set of transitions, i.e., defined by  $((q, s_h, s_s), (q', s'_h, s'_s)) \in \Delta_{\mathcal{P}}$  if and only if  $(q, q') \in \delta$ ,  $\exists l_h \in 2^{\Pi_h}$  and  $\exists l_s \in 2^{\Pi_s}$  such that  $s'_h \in \Delta(s_h, l_h)$  and  $s'_s \in \Delta(s_s, l_s)$ ;
- $h_{\mathcal{P}} : \Delta_{\mathcal{P}} \rightarrow \{0, \infty\}$ ;
- $\omega_{\mathcal{P}} : \Delta_{\mathcal{P}} \rightarrow \mathbb{R}^+$  is the weight function;
- $v_{\mathcal{P}} : \Delta_{\mathcal{P}} \rightarrow \mathbb{R}^+$  is the violation function;
- $\mathcal{F}_{\mathcal{P}} = Q \times \mathcal{F}_h \times \mathcal{F}_s$  is the set of accepting states.

The major difference between  $\tilde{\mathcal{P}}$  and  $\mathcal{P}$  is that for two any state  $s_{\mathcal{P}} = (q, s_h, s_s)$  and  $s'_{\mathcal{P}} = (q', s'_h, s'_s)$ , the constraints  $s'_h \in \Delta(s_h, L(q))$  and  $s'_s \in \Delta(s_s, L(q))$  in  $\tilde{\mathcal{P}}$  are relaxed in  $\mathcal{P}$  as defined above. Consequently,  $\mathcal{P}$  is more connected than  $\tilde{\mathcal{P}}$  in terms of possible transitions, which will reduce the computational complexity during automaton update (see Section IV-C). Any transition  $((q, s_h, s_s), (q, s'_h, s'_s)) \in \Delta_{\mathcal{P}}$  that violates the hard constraint will have a infinite violation  $h_{\mathcal{P}}(((q, s_h, s_s), (q, s'_h, s'_s)))$ . To identify trajectories that violate the original  $\phi_s$  the least when the environment is

infeasible,  $v_P$  is designed to quantify the violation cost. Suppose that  $\Pi = \{\alpha_1, \alpha_2 \dots \alpha_M\}$  and consider an evaluation function  $\text{Eval}: 2^\Pi \rightarrow \{0, 1\}^M$ , where  $\text{Eval}(l) = (v_i)^M$  with  $v_i = 1$  if  $\alpha_i \in l$  and  $v_i = 0$  if  $\alpha_i \notin l$ , where  $i = 1, 2, \dots, M$  and  $l \in 2^\Pi$ . To quantify the difference between two elements in  $2^\Pi$ , consider  $\rho(l, l') = \|v - v'\|_1 = \sum_{i=1}^M |v_i - v'_i|$ , where  $v = \text{Eval}(l)$ ,  $v' = \text{Eval}(l')$ ,  $l, l' \in 2^\Pi$ , and  $\|\cdot\|_1$  is the  $l_1$  norm. The distance from  $l \in 2^\Pi$  to a set  $\mathcal{X} \subseteq 2^\Pi$  is then defined as  $\text{Dist}(l, \mathcal{X}) = \min_{l' \in \mathcal{X}} \rho(l, l')$  if  $l \notin \mathcal{X}$ , and  $\text{Dist}(l, \mathcal{X}) = 0$  otherwise. Now the violation cost of the transition from  $s_P = (q, s_h, s_s)$  to  $s'_P = (q', s'_h, s'_s)$  can be defined as  $v_P(s_P, s'_P) = \text{Dist}(L(q), \mathcal{X}(s_s, s'_s))$ , where  $\mathcal{X}(s_s, s'_s) = \{l \in 2^\Pi | s'_s \in \Delta(s_s, l)\}$  is the set of input alphabets that enables the transition from  $s_s$  to  $s'_s$ . Hence, the violation cost  $v_P(s_P, s'_P)$  quantifies how much the transition from  $s_P$  to  $s'_P$  in  $\mathcal{P}$  violates the constraints imposed by  $\phi_s$ .

Based on the defined  $v_P(s_P, s'_P)$ , we design the weight function  $\omega_P(s_P, s'_P) = h_P(s_P, s'_P) + \omega(q, q') + \beta \cdot v_P(s_P, s'_P)$ , where  $\beta \in \mathbb{R}^+$  indicates the relative penalty. A larger  $\beta$  tends to bias the selection of trajectories with less violation cost. The weight function  $\omega(q, q')$  is defined on the Euclidean distance between  $q$  and  $q'$  on  $\mathcal{T}$ , which measures the implementation cost of the transition from  $q$  to  $q'$ . Since each transition  $(s_k^P, s_{k+1}^P) \in \Delta_P$  is associated with a weight in Def. 4, the total weight of a trajectory  $s_P$  is

$$\mathcal{W}(s_P) = \sum_{k=1}^{n-1} (h_P(s_k^P, s_{k+1}^P) + \omega(q_k, q_{k+1}) + \beta \cdot v_P(s_k^P, s_{k+1}^P)). \quad (1)$$

**Theorem 1.** *Given an accepting run  $s_P = (q_0, s_{h0}, s_{s0})(q_1, s_{h1}, s_{s1}) \dots$  of  $\mathcal{P}$  for  $\phi = \phi_h \wedge \phi_s$ , the hard constraints  $\phi_h$  will always be satisfied if  $\mathcal{W}(s_P) \neq \infty$ .*

*Proof:* Let  $\mathcal{F}_h$  denote the set of accepting states of  $\mathcal{B}_h$  corresponding to  $\mathcal{F}_P$  (i.e., the projection of  $\mathcal{F}_P$  of  $\mathcal{P}$  onto  $\mathcal{F}_h$  of  $\mathcal{B}_h$ ), and let  $s_h = s_{h0}s_{h1} \dots$  denote the projection of  $s_P$  over  $\mathcal{P}$  onto  $\mathcal{B}_h$ . By the definition of an accepting run,  $s_P$  intersects at least one state of  $\mathcal{F}_P$  infinitely often, which implies  $s_h$  visits  $\mathcal{F}_h$  infinitely often. In addition, by the definition of  $\Delta_P \subseteq \mathcal{S}_P \times \mathcal{S}_P$ , all transitions along  $s_h$  follow the rule  $s_{hi} \xrightarrow{L(q)} s_{hj}$  if  $h_P(s_{pi}, s_{pj}) = 0$ , which implies the transitions are always valid in  $\mathcal{B}_h$ . Therefore,  $s_h$  satisfies the accepting conditions of  $\mathcal{B}_h$ , which implies that  $\phi_h$  is fully satisfied. ■

Theorem 1 indicates that any accepting run of  $\mathcal{P}$  can guarantee that the hard constraints  $\phi_h$  are satisfied by selecting the run with finite total cost in (1). An accepting run  $s_P$  is valid if and only if it satisfies  $\phi_h$ . In (1), the term  $\sum_{k=1}^{n-1} \beta \cdot v_P(s_k^P, s_{k+1}^P)$  measures the violation of  $\phi_s$ . Hence, a valid accepting run  $s_P$  fulfills  $\phi_s$  as much as possible, if the violation of  $\phi_s$  can be minimized.

**Example 1.** Consider an example of  $\phi = \phi_h \wedge \phi_s$  and  $\mathcal{T}$  in Fig. 2. The double circles in Fig. 2(a) and (b) represent the accepting states of  $\mathcal{B}_h$  and  $\mathcal{B}_s$ , respectively. Fig. 2(a) represents safety constraints of avoiding obstacles and Fig.

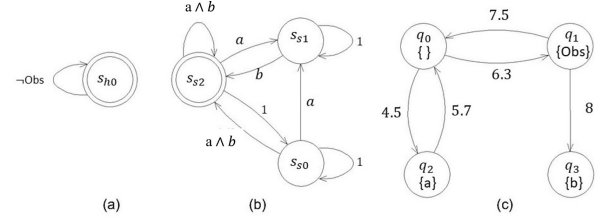


Figure 2: (a) Example of safety constraint  $\phi_h = \neg \text{Obs}$ . (b) Example of a soft constraint  $\phi_s = \diamond a \vee \diamond b$ . (c) Example of DTS.

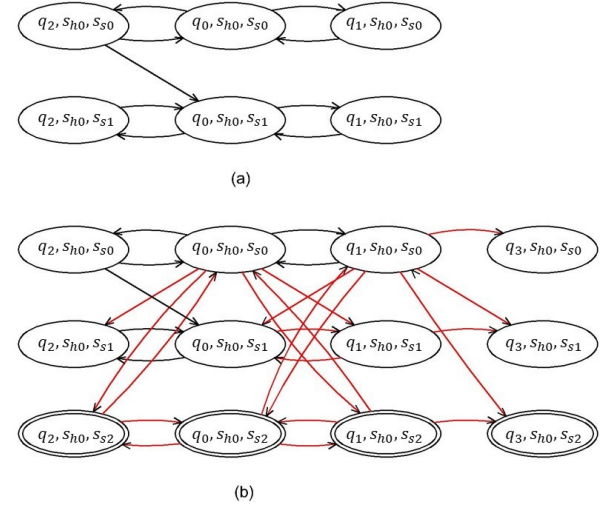


Figure 3: (a) Product automaton based on Def.3. (b) Relaxed product automaton based on Def.4.

2(b) represents soft constraints of visiting  $a$  and  $b$  infinitely often. Fig. 2(c) represents a DTS with labeled states. Fig. 3(a) shows the product automaton in Def. 3 between  $\mathcal{T}$  and the two NAB  $\phi_h$  and  $\phi_s$ . Fig. 3(b) shows the relaxed product automaton in Def. 4, where red edges represent transitions with non-zero violation cost. The plot in Fig. 3 omits the states that are not reachable from initial states and double circle states are accepting states. In Fig. 3(a), there exists no accepting path since accepting states are not reachable due to constraints of  $\phi_h$ . In contrast, in the relaxed automaton, there exists a path visiting accepting states infinitely often. In this case, the projection of accepting path with minimum violation cost in Fig. 3(b) onto DTS  $\mathcal{T}$  is the path visiting  $a$  of Fig. 2(c) infinitely often while avoiding obstacles.

*Remark 1.* Since the accepting condition of  $\mathcal{P}$  requires to visit both accepting states of  $\mathcal{B}_h$  and  $\mathcal{B}_s$  infinitely, there should exist no conflicts between the satisfaction of  $\mathcal{B}_h$  and  $\mathcal{B}_s$  in this work and [46]. The more general construction without considering such conflicts can be found in [12] resulting extra dimensional complexity and our framework also works for the general design.

### B. Energy Function

Analogous to Lyapunov theory, where the convergence of the system states to equilibrium points is indicated by a decreasing Lyapunov function, a Lyapunov-like energy function is designed in this section to enforce the acceptance condition of an automaton by requiring the distance to the accepting states to decrease as the system evolves. Given two states  $s_i^P, s_j^P \in S_P$ , the set of all finite trajectories on  $\mathcal{P}$  from  $s_i^P$  to  $s_j^P$  is defined as  $\mathcal{D}(s_i^P, s_j^P) = \{s_P = s_1^P s_2^P \dots s_n^P\}$  such that  $s_1^P = s_i^P, s_n^P = s_j^P, (s_k^P, s_{k+1}^P) \in \Delta_P, \forall k = 1, 2, \dots, n-1$ . If  $\mathcal{D}(s_i^P, s_j^P) \neq \emptyset$ ,  $s_j^P$  is reachable from  $s_i^P$  on  $\mathcal{P}$ . Based on (1), the distance  $d(s_i^P, s_j^P)$  is defined as the lowest total weight along a trajectory from  $s_i^P$  to  $s_j^P$ , i.e.,

$$d(s_i^P, s_j^P) = \begin{cases} \min_{s_P \in \mathcal{D}(s_i^P, s_j^P)} \mathcal{W}(s_P) & \text{if } \mathcal{D}(s_i^P, s_j^P) \neq \emptyset, \\ \infty & \text{Otherwise.} \end{cases} \quad (2)$$

$d(s_i^P, s_j^P)$  can be efficiently determined by the well known Dijkstra's algorithm.

Given  $\mathcal{P}_{(S_P, \Delta_P)}$ , the graph induced from  $\mathcal{P}_{(S_P, \Delta_P)}$  by neglecting the weight of each transition is denoted by  $\mathcal{G}_{(S_P, \Delta_P)}$ .

**Definition 5.** The largest self-reachable subset of the accepting set  $\mathcal{F}_P$  is defined as  $\mathcal{F}^*$  such that each pair states of  $\mathcal{F}^*$  can reach each other in  $\mathcal{P}$ .

$\mathcal{F}^*$  in this paper can be constructed by following similar procedures in [24] by neglecting the cost of  $h_P$ .

**Definition 6 (Energy Function).** For  $s_P \in S_P$ , the energy function  $J(s_P)$  is designed as

$$J(s_P) = \begin{cases} \min_{s'_P \in \mathcal{F}^*} d(s_P, s'_P) & \text{if } s_P \notin \mathcal{F}^*, \\ 0 & \text{if } s_P \in \mathcal{F}^*. \end{cases} \quad (3)$$

The design of  $J(s_P)$  in (6) is inspired by [24]. Different from [24], we adapt it to the relaxed product automaton by taking into account the distance from the states to the largest self-reachable subset  $\mathcal{F}^*$  of the relaxed product automaton. Since  $\omega_P$  is positive by definition,  $d(s_P, s'_P) > 0$  for all  $s_P, s'_P \in S_P$ , which implies that  $J(s_P) \geq 0$ . Particularly,  $J(s_P) = 0$  if  $s_P \in \mathcal{F}^*$ . If a state in  $\mathcal{F}^*$  is reachable from  $s_P$ , then  $J(s_P) \neq \infty$ , otherwise  $J(s_P) = \infty$ . Hence,  $J(s_P)$  indicates the minimum distance from  $s_P$  to  $\mathcal{F}^*$ .

**Theorem 2.** For the energy function designed in (3), if a trajectory  $s_P = s_1^P s_2^P \dots s_n^P$  is accepting, there is no state  $s_i^P, \forall i = 1, \dots, n$ , with  $J(s_i^P) = \infty$ , and all accepting states in  $s_P$  are in the set  $\mathcal{F}^*$  with energy 0. In addition, for any state  $s_P \in S_P$  with  $s_P \notin \mathcal{F}^*$  and  $J(s_P) \neq \infty$ , there exists at least one state  $s'_P$  with  $(s_P, s'_P) \in \Delta_P$  such that  $J(s'_P) < J(s_P)$ .

*Proof:* Consider an accepting state  $s_i^P \in \mathcal{F}_P$ . Suppose  $s_i^P \notin \mathcal{F}^*$ . If a trajectory  $s_P$  is accepting,  $s_P$  must intersect  $\mathcal{F}_P$  infinitely many times by Def. 4, which indicates there exists another state  $s_j^P \in \mathcal{F}_P$  such that  $s_j^P$  is reachable from  $s_i^P$ . If  $s_j^P \in \mathcal{F}^*$ , the construction of  $\mathcal{F}^*$  indicates that  $s_i^P$  must be in  $\mathcal{F}^*$ , which contradicts the assumption that  $s_i^P \notin \mathcal{F}^*$ . If

$s_j^P \notin \mathcal{F}^*$ , there must exist a non-trivial strongly connected component (SCC) composed of accepting states reachable from  $s_j^P$  [42]. By definition of  $\mathcal{F}^*$ , all states in SCC belong to  $\mathcal{F}^*$ . Since the SCC is reachable from  $s_j^P$ , it implies  $s_j^P \in \mathcal{F}^*$ , which contradicts that  $s_j^P \notin \mathcal{F}^*$ . Consequently, all accepting states in  $s_P$  must be in  $\mathcal{F}^*$  and have energy zero based on (3). Since  $\mathcal{F}^*$  is reachable by any state in  $s_P$ ,  $J(s_i^P) \neq \infty$  for all  $i = 1, \dots, n$ .

If  $J(s_P) \neq \infty$  for  $s_P \in S_P$ , (3) indicates  $\mathcal{F}^*$  is reachable strictly following the hard constraint from  $s_P$ . That is, based on the distance defined in (2), there exists a shortest trajectory  $s_P = s_1^P s_2^P \dots s_n^P$ , where  $s_1^P = s_P$  and  $s_n^P \in \mathcal{F}^*$ . Bellman's optimal principle can then be invoked to conclude that there exists a state  $s'_P$  with  $(s_P, s'_P) \in \Delta_P$  such that  $J(s'_P) < J(s_P)$ . ■

Theorem 2 indicates that, as long as the energy function keeps decreasing, the generated trajectory will eventually satisfy the accepting conditions in Def. 4. As a result, the designed energy function can be used to enforce the convergence to accepting states.

### C. Automaton Update

Since the environment is only partially known, this section describes how the real-time information sensed by the robot during the runtime can be used to update the system model to facilitate motion planning. The robot starts with an initial, possibly imprecise, knowledge about the environment. A potential cause of infeasible task specifications is the imprecise state labels. Due to limited local sensing capability, let  $Q_N$  denote the set of sensible neighboring states and let  $\llbracket s_P \rrbracket = \{s_P = (q, s_h, s_s) \mid q \in Q_N\}$  denote a class of  $s_P$  sharing the same neighboring states. Specifically, let  $\text{Info}(s_P) = \{L_P(s'_P) \mid s'_P \in \text{Sense}(s_P)\}$  denote the newly observed labels of  $s'_P$  that are different from the current knowledge, where  $\text{Sense}(s_P)$  represents a local set of states that can be sensed by the robot at  $s_P$ . If the sensed labels  $L_P(s'_P)$  are consistent with the current knowledge of  $s'_P$ ,  $\text{Info}(s_P) = \emptyset$ . Otherwise, the properties of  $s'_P$  need to be updated.

Let  $\mathbf{J}(\llbracket s_P \rrbracket) \in \mathbb{R}^{\llbracket s_P \rrbracket}$  denote the stacked  $J$  for all  $s_P \in \llbracket s_P \rrbracket$ . For  $i, j = 1, \dots, |S_P|$ , let  $\mathbf{H}_P \in \mathbb{R}^{|S_P| \times |S_P|}$  denote a matrix where the  $(i, j)$ th entry of  $\mathbf{H}_P$  represents  $h_P(s_i^P, s_j^P)$  and let  $\mathbf{V}_P \in \mathbb{R}^{|S_P| \times |S_P|}$  denote a matrix where the  $(i, j)$ th entry of  $\mathbf{V}_P$  represents the violation cost  $v_P(s_i^P, s_j^P)$ . The terms  $\mathbf{J}$ ,  $\mathbf{H}_P$  and  $\mathbf{V}_P$  are initialized from the initial knowledge of the environment. Algorithm 1 outlines how  $\mathbf{H}_P$ ,  $\mathbf{V}_P$  and  $\mathbf{J}$  are updated based on the locally sensed information to facilitate motion planning in line 2-9. At each step, if  $\text{Info}(s_P) \neq \emptyset$ , the energy function  $\mathbf{J}$  for each states of  $\llbracket s_P \rrbracket$  is updated by Algorithm 1.

**Lemma 1.** The largest self-reachable set  $\mathcal{F}^*$  remains the same during the automaton update in Algorithm 1.

*Proof:* By neglecting the cost of transitions in Section IV-B, the relaxed product automaton  $\mathcal{P}_{(S_P, \Delta_P)}$  can be treated as a directed graph  $\mathcal{G}_{(S_P, \Delta_P)}$ . By Def.4, Alg. 1 only updates the cost of each transition. As a result, the topological structure of  $\mathcal{G}_{(S_P, \Delta_P)}$  and its corresponding  $\mathcal{F}^*$  remain the same. ■



**Algorithm 1** Automaton Update

---

```

1: procedure INPUT: ( the current state  $s_{\mathcal{P}} = (q, s_h, s_s)$ , the current  $J(\llbracket s_{\mathcal{P}} \rrbracket)$ ,
    $\mathcal{F}^*$ , and  $\text{Info}(s_{\mathcal{P}})$ )
   Output: the updated  $\mathcal{J}'$ 
2: if  $\text{Info}(s_{\mathcal{P}}) \neq \emptyset$  then
3:   for all  $s'_{\mathcal{P}} = (q', s'_h, s'_s) \in \text{Sense}(s_{\mathcal{P}})$  such that  $L_{\mathcal{P}}(s'_{\mathcal{P}}) \in \text{Info}(s_{\mathcal{P}})$  do
4:     for all  $s'_{\mathcal{P}}$  such that  $(s'_{\mathcal{P}}, s'_{\mathcal{P}}) \in \Delta_{\mathcal{P}}$  do
5:       Update the labels of  $L_{\mathcal{P}}(s'_{\mathcal{P}})$  according to  $L(q')$ 
6:       Update  $\mathbf{H}_{\mathcal{P}}$  and  $\mathbf{V}_{\mathcal{P}}$ 
7:     end for
8:   end for
9:   Update  $J(\llbracket s_{\mathcal{P}} \rrbracket)$  based on (3)
10: end if
11: end procedure

```

---

*Remark 2.* The construction of  $\mathcal{F}^*$  in [24] involves the computation of  $d(s_{\mathcal{P}}, s'_{\mathcal{P}})$  for all  $s'_{\mathcal{P}} \in \mathcal{F}_{\mathcal{P}}$  and the check of terminal conditions, leading to the computational complexity of  $O(|\mathcal{F}_{\mathcal{P}}|^3 + |S_{\mathcal{P}}|^2 \times |\mathcal{F}_{\mathcal{P}}|^2 + |\mathcal{F}_{\mathcal{P}}|)$ . In contrast, Lemma 1 indicates that  $\mathcal{F}^*$  in this work only needs to be updated whenever newly sensed information different from its knowledge is obtained, which reduces the complexity. In the worst case, the complexity is  $|Q_N|$ . Instead of computing the whole relaxed product automaton, Algorithm 1 only updates partial information of the systems.

## V. CONTROL SYNTHESIS OF LTL MOTION PLANNING

This section presents a RHC-based online motion planning strategy that optimizes accumulated utilities over a predefined finite horizon subject to energy function based constraints, where the accumulated utilities take into account both the time-varying reward and the violation cost, while the energy function based constraints enforce the satisfaction of the acceptance condition of the relaxed product automaton  $\mathcal{P}$ .

## A. Receding Horizon Control

The general idea of RHC is to generate a predicted optimal trajectory at each time step by solving an online optimization problem to maximize a utility function over a finite horizon  $N$ . With only the first predicted step applied, the optimization problem is repeatedly solved to predict optimal trajectories. Specifically, based on the current state  $s_k^{\mathcal{P}}$ , let  $\bar{s}_k^{\mathcal{P}} = s_{1|k}^{\mathcal{P}} s_{2|k}^{\mathcal{P}} \dots s_{N|k}^{\mathcal{P}}$  denote a predicted trajectory of horizon  $N$  at time  $k$  from  $s_k^{\mathcal{P}}$ , where the  $i$ th predicted state  $s_{i|k}^{\mathcal{P}} \in S_{\mathcal{P}}$  satisfies  $(s_{i|k}^{\mathcal{P}}, s_{i+1|k}^{\mathcal{P}}) \in \Delta_{\mathcal{P}}$  for all  $i = 1, \dots, N-1$ , and  $(s_k^{\mathcal{P}}, s_{1|k}^{\mathcal{P}}) \in \Delta_{\mathcal{P}}$ . Let  $\text{Path}(s_k^{\mathcal{P}}, N)$  be the set of trajectories of horizon  $N$  generated from  $s_k^{\mathcal{P}}$ . Note that a predicted trajectory  $\bar{s}_k^{\mathcal{P}} \in \text{Path}(s_k^{\mathcal{P}}, N)$  can uniquely project to a path  $\gamma_{\mathcal{T}}(\bar{s}_k^{\mathcal{P}}) = \mathbf{q} = q_1 \dots q_N$  on  $\mathcal{T}$ , where  $\gamma_{\mathcal{T}}(s_{i|k}^{\mathcal{P}}) = q_i$ ,  $\forall i = 1, \dots, N$ .

The finite horizon  $N$  is selected based on the robot's local sensing such that the labels  $L_{\mathcal{P}}(q_i)$  and the reward  $R_k(q_i)$ ,  $\forall i = 1, \dots, N$ , are all observable by the robot at time  $k$ . The accumulated reward along the predicted trajectory  $\bar{s}_k^{\mathcal{P}}$  is  $\mathbf{R}(\gamma_{\mathcal{T}}(\bar{s}_k^{\mathcal{P}})) = \sum_{i=1}^N R_k(\gamma_{\mathcal{T}}(s_{i|k}^{\mathcal{P}}))$ .

Once a predicted step  $k$  of RHC is implemented, the hard and soft violation cost induced from the current state  $s_k^{\mathcal{P}}$  to the next predicted step  $s_{1|k}^{\mathcal{P}}$  are considered, i.e.,  $h_{\mathcal{P}}(s_k^{\mathcal{P}}, s_{1|k}^{\mathcal{P}})$  and  $\mathbf{V}(s_k^{\mathcal{P}}) = \beta \cdot v_{\mathcal{P}}(s_k^{\mathcal{P}}, s_{1|k}^{\mathcal{P}})$ . The utility function of RHC is then designed as

$$\mathbf{U}(\bar{s}_k^{\mathcal{P}}) = -h_{\mathcal{P}}(s_k^{\mathcal{P}}, s_{1|k}^{\mathcal{P}}) + \mathbf{R}(\gamma_{\mathcal{T}}(\bar{s}_k^{\mathcal{P}})) \min \left\{ e^{-\kappa \mathbf{V}(s_k^{\mathcal{P}})}, 1 \right\} \quad (4)$$

where  $\kappa \in \mathbb{R}^+$  is a tuning parameter indicating how aggressively a predicted path is penalized by violating the soft task constraints and the non-zero violation  $\mathbf{V}(s_k^{\mathcal{P}})$  in (4) would enforce the decrease of  $\mathbf{U}(\bar{s}_k^{\mathcal{P}})$ . If  $h_{\mathcal{P}}(s_k^{\mathcal{P}}, s_{1|k}^{\mathcal{P}}) = \infty$ , it indicates that  $\mathbf{U}(\bar{s}_k^{\mathcal{P}})$  is negative infinite. By applying a larger  $\kappa$  optimizing  $\mathbf{U}(\bar{s}_k^{\mathcal{P}})$  tends to bias the selection of paths towards the objectives, in the decreasing order, of 1) hard task  $\phi_h$  satisfaction, 2) fulfilling soft task  $\phi_s$  as much as possible, and 3) time-varying rewards locally optimization.

Since maximizing  $\mathbf{U}(\bar{s}_k^{\mathcal{P}})$  alone cannot guarantee the satisfaction of the acceptance condition of  $\mathcal{P}$ , energy function the energy function based constraints are incorporated. We first select initial states from  $S_{\mathcal{P}0}$  that can reach the set  $\mathcal{F}^*$ . The RHC executing on  $S_{\mathcal{P}0}$  is designed as

$$\begin{aligned} \bar{s}_{0,\text{opt}}^{\mathcal{P}} &= \arg \max_{\bar{s}_0^{\mathcal{P}} \in \text{Path}(s_0^{\mathcal{P}}, N)} \mathbf{U}(\bar{s}_0^{\mathcal{P}}) \\ &\text{subject to : } J(s_0^{\mathcal{P}}) < \infty. \end{aligned} \quad (5)$$

The constraint  $J(s_0^{\mathcal{P}}) < \infty$  in (5) is critical, since a bounded energy  $J(s_0^{\mathcal{P}})$  guarantees the existence of a satisfying trajectory from  $s_0^{\mathcal{P}}$  over  $\mathcal{P}$ . According to the working principle of RHC, the first element of the optimal trajectory  $\bar{s}^{\mathcal{P}*}$  can be determined as  $s_0^{\mathcal{P}*} = s_{1|0,\text{opt}}^{\mathcal{P}}$ , where  $s_{1|0,\text{opt}}^{\mathcal{P}}$  is the first element of  $\bar{s}_{0,\text{opt}}^{\mathcal{P}}$  obtained from (5).

After determining the initial state  $s_0^{\mathcal{P}*}$ , RHC will be employed repeatedly to determine the optimal states  $s_k^{\mathcal{P}*}$  for  $k = 1, 2, \dots$ . At each time instant  $k$ , a predicted optimal trajectory  $\bar{s}_{k,\text{opt}}^{\mathcal{P}} = s_{1|k,\text{opt}}^{\mathcal{P}} s_{2|k,\text{opt}}^{\mathcal{P}} \dots s_{N|k,\text{opt}}^{\mathcal{P}}$  will be constructed based on  $s_{k-1}^{\mathcal{P}*}$  and  $\bar{s}_{k-1,\text{opt}}^{\mathcal{P}}$  obtained at the previous time  $k-1$ . Note that only  $s_{1|k,\text{opt}}^{\mathcal{P}}$  will be applied at time  $k$ , i.e.,  $s_k^{\mathcal{P}*} = s_{1|k,\text{opt}}^{\mathcal{P}}$ , which will then be used with  $\bar{s}_{k,\text{opt}}^{\mathcal{P}}$  to generate  $\bar{s}_{k+1,\text{opt}}^{\mathcal{P}}$ .

**Theorem 3.** For each time  $k = 1, 2, \dots$ , provided  $s_{k-1}^{\mathcal{P}*}$  and  $\bar{s}_{k-1,\text{opt}}^{\mathcal{P}}$  from previous time step, consider a receding horizon control (RHC)

$$\bar{s}_{k,\text{opt}}^{\mathcal{P}} = \arg \max_{\bar{s}_k^{\mathcal{P}} \in \text{Path}(s_{k-1}^{\mathcal{P}*}, N)} \mathbf{U}(\bar{s}_k^{\mathcal{P}}) \quad (6)$$

subject to the following constraints:

- 1)  $J(s_{N|k}^{\mathcal{P}}) < J(s_{N|k-1,\text{opt}}^{\mathcal{P}})$  if  $J(s_{k-1}^{\mathcal{P}*}) > 0$  and  $J(s_{i|k-1,\text{opt}}^{\mathcal{P}}) \neq 0$  for all  $i = 1, \dots, N$ ;
- 2)  $J(s_{i_0(s_{k-1}^{\mathcal{P}*})-1|k}^{\mathcal{P}}) = 0$  if  $J(s_{k-1}^{\mathcal{P}*}) > 0$  and  $J(s_{i|k-1,\text{opt}}^{\mathcal{P}}) = 0$  for some  $i = 1, \dots, N$ ;
- 3)  $J(s_{N|k}^{\mathcal{P}}) < \infty$  if  $J(s_{k-1}^{\mathcal{P}*}) = 0$ .

Applying  $s_k^{\mathcal{P}*} = s_{1|k,\text{opt}}^{\mathcal{P}}$  at each time  $k$ , the optimal trajectory

$\bar{s}^{\mathcal{P}^*} = s_0^{\mathcal{P}^*} s_1^{\mathcal{P}^*} \dots$  is guaranteed to satisfy the acceptance condition of  $\mathcal{P}$ .

*Proof:* Consider a state  $s_{k-1}^{\mathcal{P}^*} \in S_{\mathcal{P}}$ ,  $\forall k = 1, 2, \dots$ , and  $\text{Path}(s_{k-1}^{\mathcal{P}^*}, N)$  represents the set of all possible paths starting from  $s_{k-1}^{\mathcal{P}^*}$  with horizon  $N$ . Since not all predicated trajectories maximizing the utility  $\mathbf{U}(\bar{s}_k^{\mathcal{P}})$ ,  $\bar{s}_k^{\mathcal{P}} \in \text{Path}(s_{k-1}^{\mathcal{P}^*}, N)$ , in (6) are guaranteed to be accepting by  $\mathcal{P}$ , additional constraints need to be imposed. Note that the energy function  $J(s_{k-1}^{\mathcal{P}^*})$  defined in (3) indicates the distance from the current state  $s_{k-1}^{\mathcal{P}^*}$  to  $\mathcal{F}^*$ . A trajectory on  $\mathcal{P}$  is accepting if the trajectory can intersect  $\mathcal{F}^*$  infinitely many times. Therefore, the key idea of the design of the constraints for (6) is to ensure the energy of the states along the trajectory eventually decreases to zero. Following this idea, different cases are considered.

(i) Case 1: If  $J(s_{k-1}^{\mathcal{P}^*}) > 0$  and  $J(s_{i|k-1, \text{opt}}^{\mathcal{P}}) \neq 0$  for all  $i = 1, \dots, N$ , the constraint  $J(s_{N|k}^{\mathcal{P}}) < J(s_{N|k-1, \text{opt}}^{\mathcal{P}})$  is enforced. Recall that  $\bar{s}_{k-1, \text{opt}}^{\mathcal{P}} = s_{1|k-1, \text{opt}}^{\mathcal{P}} s_{2|k-1, \text{opt}}^{\mathcal{P}} \dots s_{N|k-1, \text{opt}}^{\mathcal{P}}$  is the predicted optimal trajectory at the previous time  $k-1$ . The energy  $J(s_{k-1}^{\mathcal{P}^*}) > 0$  indicates that there exists a trajectory from  $s_{k-1}^{\mathcal{P}^*}$  to  $\mathcal{F}^*$ , and  $J(s_{i|k-1, \text{opt}}^{\mathcal{P}}) \neq 0$  for all  $i = 1, \dots, N$  indicates  $\bar{s}_{k-1, \text{opt}}^{\mathcal{P}}$  does not intersect  $\mathcal{F}^*$ . The constraint  $J(s_{N|k}^{\mathcal{P}}) < J(s_{N|k-1, \text{opt}}^{\mathcal{P}})$  enforces that the energy of the last state  $s_{N|k}^{\mathcal{P}}$  in the predicted trajectory at the current time  $k$  must be less than that of the previously predicted  $\bar{s}_{k-1, \text{opt}}^{\mathcal{P}}$ , which indicates the energy along  $\bar{s}_{k, \text{opt}}^{\mathcal{P}}$  strictly decreases at each iteration  $k$ . Note that, based on Theorem 2, there always exists a state  $s'_{\mathcal{P}}$  on  $\mathcal{P}$  satisfying  $(s_{N|k-1, \text{opt}}^{\mathcal{P}}, s'_{\mathcal{P}}) \in \Delta_{\mathcal{P}}$  and  $J(s'_{\mathcal{P}}) < J(s_{N|k-1, \text{opt}}^{\mathcal{P}})$ . Therefore, if we can construct a trajectory  $\bar{s}_k^{\mathcal{P}} = s_{1|k}^{\mathcal{P}}, \dots, s_{N|k}^{\mathcal{P}}$  with  $s_{i|k}^{\mathcal{P}} = s_{i+1|k-1, \text{opt}}^{\mathcal{P}}$  and  $s_{N|k, \text{opt}}^{\mathcal{P}} = s'_{\mathcal{P}}$  for all  $i = 1, \dots, N-1$ , the problem (6) is guaranteed to have at least one solution for Case 1.

(ii) Case 2: If  $J(s_{i|k-1, \text{opt}}^{\mathcal{P}}) = 0$  for some  $i = 1, \dots, N$ ,  $\bar{s}_{k-1, \text{opt}}^{\mathcal{P}}$  intersects  $\mathcal{F}^*$ . Let  $i_0$  ( $\bar{s}_{k-1, \text{opt}}^{\mathcal{P}}$ ) be the index of the first occurrence in  $\bar{s}_{k-1, \text{opt}}^{\mathcal{P}}$  where  $J(s_{i_0|k-1}^{\mathcal{P}}) = 0$ . The constraint  $J(s_{i_0(s_{k-1}^{\mathcal{P}^*})-1|k}^{\mathcal{P}}) = 0$  enforces the predicted trajectory at the current time  $k$  to have energy 0 (i.e., intersect  $\mathcal{F}^*$ ), if the previously predicted trajectory  $\bar{s}_{k-1, \text{opt}}^{\mathcal{P}}$  does so. To show that the problem (6) has at least one solution for Case 2, we can always construct  $\bar{s}_k^{\mathcal{P}} = s_{1|k}^{\mathcal{P}}, \dots, s_{N|k}^{\mathcal{P}}$  by letting  $s_{i|k}^{\mathcal{P}} = s_{i+1|k-1, \text{opt}}^{\mathcal{P}}$  and  $s_{N|k}^{\mathcal{P}} = s'_{\mathcal{P}}$  for all  $i = 1, \dots, N-1$ , where  $s'_{\mathcal{P}}$  can be any state on  $\mathcal{P}$  satisfying  $(s_{N|k-1, \text{opt}}^{\mathcal{P}}, s'_{\mathcal{P}}) \in \Delta_{\mathcal{P}}$  and  $J(s'_{\mathcal{P}}) < \infty$ .

(iii) Case 3: If  $J(s_{k-1}^{\mathcal{P}^*}) = 0$ , it indicates  $s_{k-1}^{\mathcal{P}^*} \in \mathcal{F}^*$ . The constraint  $J(s_{N|k}^{\mathcal{P}}) < \infty$  only requires the predicted trajectory  $\bar{s}_k^{\mathcal{P}}$  ending at a state with bounded energy, where Cases 1 and 2 can then be applied to enforce the following sequence  $s_{k+1}^{\mathcal{P}^*} s_{k+2}^{\mathcal{P}^*} \dots$  converging to  $\mathcal{F}^*$ . To show that there always exists  $s_{N|k}^{\mathcal{P}}$  with  $J(s_{N|k}^{\mathcal{P}}) < \infty$ , note that there exists a state  $s'_{\mathcal{P}}$  satisfying  $(s_{k-1}^{\mathcal{P}^*}, s'_{\mathcal{P}}) \in \Delta_{\mathcal{P}}$  and  $J(s'_{\mathcal{P}}) < \infty$ . Let  $s_{1|k}^{\mathcal{P}} = s'_{\mathcal{P}}$ . Based on Theorem 2, we can always construct

$\bar{s}_k^{\mathcal{P}} = s_{1|k}^{\mathcal{P}}, \dots, s_{N|k}^{\mathcal{P}}$  such that  $J(s_{i|k}^{\mathcal{P}}) < J(s_{i+1|k}^{\mathcal{P}})$  for all  $i = 1, \dots, N-1$ , and  $J(s_{N|k}^{\mathcal{P}}) < \infty$ . Consequently, the problem (6) has solutions for Case 3. ■

Analogous to the analysis in [24], the energy function based constraints (6) in Theorem 3 ensure that  $\bar{s}^{\mathcal{P}^*} = s_0^{\mathcal{P}^*} s_1^{\mathcal{P}^*} \dots$  intersects the accepting states  $\mathcal{F}_{\mathcal{P}}$  infinitely, resulting in the satisfaction of the acceptance condition of  $\mathcal{P}$ . If the RHC yields a negative infinite utility, the hard constraint is violated and the robot fails to accomplish the task. In this paper, we assume  $\phi_h$  is always feasible.

## B. Control Synthesis

The control synthesis of the LTL online motion planning strategy is outlined in Algorithm 2. In Lines 1-3, an off-line computation is first performed over  $\mathcal{P}$  to obtain an initial  $\mathbf{J}$  and an initial violation cost  $\mathbf{V}_{\mathcal{P}}$ . At time  $k = 0$ , the receding horizon control (5) is applied to determine  $s_0^{\mathcal{P}^*}$  in Lines 4-7. Due to the dynamic and uncertain nature of the environment, Algorithm 1 is applied at each time  $k > 0$  to update  $\mathbf{J}(\llbracket s_{\mathcal{P}} \rrbracket)$  and  $\mathbf{V}_{\mathcal{P}}$  based on local sensing in Lines 9-10. The RHC (6) is then employed based on the previously determined  $s_{k-1}^{\mathcal{P}^*}$  to generate  $\bar{s}_{k, \text{opt}}^{\mathcal{P}}$ , where the next state is determined as  $s_k^{\mathcal{P}^*} = s_{1|k, \text{opt}}^{\mathcal{P}}$  in Lines 11-12. The transition from  $s_{k-1}^{\mathcal{P}^*}$  to  $s_k^{\mathcal{P}^*}$  is then immediately applied on  $\mathcal{P}$ , which corresponds to the movement of the robot at time  $k$  from  $\gamma_{\mathcal{T}}(s_{k-1}^{\mathcal{P}^*})$  to  $\gamma_{\mathcal{T}}(s_k^{\mathcal{P}^*})$  on  $\mathcal{T}$  in Line 13. Repeating the process can generate a trajectory  $\bar{s}^{\mathcal{P}^*} = s_0^{\mathcal{P}^*} s_1^{\mathcal{P}^*} \dots$  that optimizes the utilities while satisfying the acceptance condition of  $\mathcal{P}$ . If  $J(s_0^{\mathcal{P}^*}) = \infty$ , there exists no trajectory that satisfies  $\phi_h$  in Line 17.

**Theorem 4** (Correctness of Algorithm 2). *Given a weighted DTS  $\mathcal{T} = \{Q, q_0, \delta, \Pi, L, \omega\}$  and  $\mathcal{B}_h$  and  $\mathcal{B}_s$  corresponding to  $\phi_h$  and  $\phi_s$ , respectively, if there exists an initial state  $s_0^{\mathcal{P}^*} \in S_{\mathcal{P}^*}$  with  $J(s_0^{\mathcal{P}^*}) < \infty$ , the trajectory generated by Algorithm 2 is guaranteed to satisfy the acceptance condition of  $\mathcal{P}$ .*

*Proof:* The existence of an initial state  $s_0^{\mathcal{P}^*} \in S_{\mathcal{P}^*}$  with  $J(s_0^{\mathcal{P}^*}) < \infty$  indicates the existence of a solution to (5). The solution  $\bar{s}_{0, \text{opt}}^{\mathcal{P}}$  from (5) determines the first element of the trajectory  $\bar{s}^{\mathcal{P}^*}$ , i.e.,  $s_0^{\mathcal{P}^*} = s_{1|0, \text{opt}}^{\mathcal{P}}$ , with  $J(s_0^{\mathcal{P}^*}) < \infty$ , from which (6) can be applied recursively to determine the rest elements  $s_k^{\mathcal{P}^*}$ ,  $k = 1, \dots$ , of  $\bar{s}^{\mathcal{P}^*}$ . Particularly, for each time  $k$ , if the constraint 1 in Theorem 3 is satisfied,  $J(s_{k-1}^{\mathcal{P}^*}) < \infty$  indicates there exist other states with lower energy by Theorem 2. Hence, repeatedly applying (6) can generate a set of predicted optimal paths with  $J(s_{N|k}^{\mathcal{P}}) > J(s_{N|k+1}^{\mathcal{P}}) > J(s_{N|k+2}^{\mathcal{P}}) \dots$  satisfying  $J(s_{N|j}^{\mathcal{P}}) = 0$  for some  $j > k$ . If the constraints 2) and 3) in Theorem 3 are satisfied, the predicted optimal trajectories  $\bar{s}_{k, \text{opt}}^{\mathcal{P}}$  from (6) will lead  $\bar{s}^{\mathcal{P}^*}$  to states with zero energy, which implies the intersections with  $\mathcal{F}^*$ . Repeating the process described above, the resulting trajectory  $\bar{s}^{\mathcal{P}^*}$  from Algorithm 2 satisfies the acceptance condition. Moreover, if  $J(s_k^{\mathcal{P}^*}) < \infty$ , it indicates there exists a run satisfying  $\phi_h$  and the violation cost  $-h_{\mathcal{P}}(s_k^{\mathcal{P}^*}, s_{1|k}^{\mathcal{P}})$  in RHC ensures the satisfaction of  $\phi_h$  since only the first predicted step is applied. ■



**Algorithm 2** Control synthesis of LTL online motion planning

---

```

1: procedure INPUT:(The DTS  $\mathcal{T} = \{Q, q_0, \delta, \Pi, L, \omega\}$  and the NBA  $\mathcal{B}_h, \mathcal{B}_s$ 
   corresponding to the user-specified LTL formula  $\phi = \phi_h \wedge \phi_s$ )
   Output: The trajectory  $\bar{s}^{\mathcal{P}*} = s_0^{\mathcal{P}*} s_1^{\mathcal{P}*} \dots$ .
   Off-line Execution:
2: Construct the relaxed product automaton  $\mathcal{P} = \mathcal{T} \times \mathcal{B}_h \times \mathcal{B}_s$ 
3: Construct  $\mathcal{F}^*$ , and initialize  $\mathbf{H}_{\mathcal{P}}, \mathbf{V}_{\mathcal{P}}$  and  $\mathbf{J}$ 
   online Execution:
4: if  $\exists s_0^{\mathcal{P}} \in S_{\mathcal{P}0} J(s_0^{\mathcal{P}}) < \infty$  then
5:   Solve (5) for  $\bar{s}_{0,\text{opt}}^{\mathcal{P}}$ 
6:    $s_0^{\mathcal{P}*} = s_{1|0,\text{opt}}^{\mathcal{P}}$  and  $k \leftarrow 1$ 
7:   while  $k > 0$  do
8:     Apply automaton update at  $s_{k-1}^{\mathcal{P}*}$  in Algorithm 1 based on local sensing
9:     Locally observe rewards  $R_k(\gamma_{\mathcal{T}}(s_{k-1}^{\mathcal{P}*}))$ 
10:    Solve (6) for  $\bar{s}_{k,\text{opt}}^{\mathcal{P}}$ 
11:    Implement corresponding transitions on  $\mathcal{P}$  and  $\mathcal{T}$ 
12:     $s_k^{\mathcal{P}*} = s_{1|k,\text{opt}}^{\mathcal{P}}$  and  $k++$ 
13:   end while
14: else
15:   There does not exist an accepting run from initial states;
16: end if
17: end procedure

```

---

**Corollary 1.** *Given a weighted DTS  $\mathcal{T} = \{Q, q_0, \delta, \Pi, L, \omega\}$ ,  $\mathcal{B}_h$  and  $\mathcal{B}_s$ , if  $\varphi_s$  is feasible, the solution of Algorithm 2 fully satisfies the task  $\varphi = \varphi_h \wedge \varphi_s$  exactly with  $\kappa$  in (4) selected sufficiently large.*

Since Corollary 1 is an immediate result of Theorem 1 and Theorem 4, its proof is omitted.

### C. Complexity

Since the off-line execution involves the computation of  $\mathcal{P}$ ,  $\mathcal{F}^*$ , the initial  $\mathbf{J}$ , and the initial  $\mathbf{V}_{\mathcal{P}}$ , its complexity is  $O(|\mathcal{F}_{\mathcal{P}}|^3 + |\mathcal{S}_{\mathcal{P}}|^2 \times |\mathcal{F}_{\mathcal{P}}|^2 + |\mathcal{F}_{\mathcal{P}}|)$ . For online execution, Since  $\mathcal{F}^*$  remains the same during mission operation, as indicated in Algorithm 1, the worst case requires  $\llbracket s_{\mathcal{P}} \rrbracket$  runs of Dijkstra's algorithm. In Algorithm 2, the selected horizon  $N$  in RHC is crucial to the complexity. Suppose the number of total transitions between states is  $|\Delta_{\delta}|$ . The complexity of recursive computation at each time step is bounded by  $|\Delta_{\delta}|^N$ . Another layer of the complexity in Algorithm 1 comes from the automaton update and the computation of energy function computation at each iteration. Suppose the number of  $\text{Sense}(s_{\mathcal{P}})$  is bounded by  $|N_1|$ , which indicates a maximum  $|N_1| \times |\mathcal{S}_{\mathcal{P}}|$  runs is required to update the violation cost  $\mathbf{V}_{\mathcal{P}}$  and the state labels. In addition, updating energy  $\mathbf{J}$  requires  $|\mathcal{S}_{\mathcal{P}}|$  runs of the Dijkstra Algorithm in each iteration. Therefore, the complexity of Algorithm 1 is at most  $O(|N_1| \times |\mathcal{S}_{\mathcal{P}}| + |\mathcal{S}_{\mathcal{P}}|)$ . Overall, the maximum complexity of the online portion of RHC is  $O(|N_1| \times |\mathcal{S}| + |\mathcal{S}_{\mathcal{P}}| + |\Delta_{\delta}|^N)$ .

In the simulation and experiment, we set the penalty parameter  $\beta = 500$  and the tuning parameter  $\kappa = 100$ . The LTL task is  $\phi = \phi_h \wedge \phi_s$ , where  $\phi_h = \square \neg \text{Obstacle}$  and  $\phi_s$  is defined in Section VI-A and VI-B, respectively.  $\phi_h$  was translated to a Büchi Automaton  $\mathcal{B}_h$  via LTL2BA [47] with  $|\mathcal{S}_h| = 1$ .

## VI. CASE STUDY

### A. Simulation Results

Consider an application in which a mobile robot performs persistent surveillance in a dynamic environment. The envi-

ronment consists of a Base station that the robot should visit repeatedly, Survey points that indicate the areas of interest that the robot should explore, a Report station where the robot should report its findings after visiting Survey, a Supply station where the robot can get refueled, and a set of Obstacle that the robot should avoid during the mission. It is assumed that the locations of Supply, Base, and Report are fixed and known to the robot, while the Survey points (i.e., the events of interest) are dynamic and can even be occasionally infeasible for the robot to explore. In addition, the potential Obstacle are dynamic. The task of the robot is formulated based on LTL as

$$\begin{aligned}
\phi_s = & \square \diamond \text{Base} \\
& \wedge \square (\text{Base} \rightarrow \circ (\neg \text{Base} \cup \text{Survey})) \\
& \wedge \square (\text{Survey} \rightarrow \circ (\neg \text{Survey} \cup \text{Report})) \\
& \wedge \square (\text{Report} \rightarrow \circ (\neg \text{Report} \cup \text{Supply})).
\end{aligned} \tag{7}$$

In English,  $\phi_s$  in (7) means the robot needs to always avoid Obstacle while repeatedly and sequentially visiting Base, Survey, Report, and Supply.

The workspace is abstracted to a grid-like graph consisting of  $10 \times 10$  nodes as shown in Fig. 4. The labels  $\Pi = \{\text{Base}, \text{Supply}, \text{Report}, \text{Obstacle}, \text{Survey}\}$  are shown in circles with blue, purple, cyan, black, and yellow, respectively. The robot is represented by a red dot transiting along edges between nodes. Each node  $q$  in the graph is associated with a time-varying reward  $R_k(q)$ , and the reward is randomly generated from a uniform distribution in the range  $[10, 25]$  at time  $k$ . The rewards are presented as green circles with size proportional to the reward value. LTL2BA [47] was used to translate  $\phi_s$  to a Büchi Automaton  $\mathcal{B}_s$  with  $|\mathcal{S}_s| = 28$  states.

The simulation was implemented in MATLAB on a PC with 3.6 GHz Quad-core CPU and 32 GB of RAM. Since the DTS  $\mathcal{T}$  has  $|Q| = 100$  states, the relaxed product automaton  $\mathcal{P}$  has  $|\mathcal{S}_{\mathcal{P}}| = 2800$  states. The computation of  $\mathcal{P}$ , the largest self-reachable set  $\mathcal{F}^*$ , and the energy function took 4.7s. The control algorithm outlined in Algorithm 2 was implemented for 200 time steps with horizon  $N = 4$ . Each iteration of Algorithm 2 took 1 to 3s depending on the volume of local updates. To demonstrate the ability of the robot in handling partially infeasible tasks, it is assumed that the  $\phi_s$  is fully feasible in the first 100 time steps and it becomes infeasible afterwards in the sense that the survey points are not accessible (i.e., yellow nodes are off).

Fig. 4(a) shows the robot's initial knowledge about the environment, which consists of known destinations  $\{\text{Base}, \text{Supply}, \text{Report}\}$  and locally observed rewards. Figs. 4(b) and (c) show the snapshots of the environment at  $t = 1\text{s}$  and  $t = 140\text{s}$ , respectively. Fig. 4(c) shows that  $\phi_s$  is relaxed since the robot is required to visit Survey points in (7), while Survey points do not exist from  $t = 101\text{s}$  to  $t = 200\text{s}$ , thus leading to a revised motion plan. Note that, due to the consideration of dynamic obstacles, the deployment of black circles can vary with time. Figs. 5(a) and (b) show the trajectories of the robot in the feasible and infeasible  $\phi_s$ , respectively. Fig. 6 shows the evolution of the energy function during mission operation. Each time the energy  $J(s_{\mathcal{P}}) = 0$

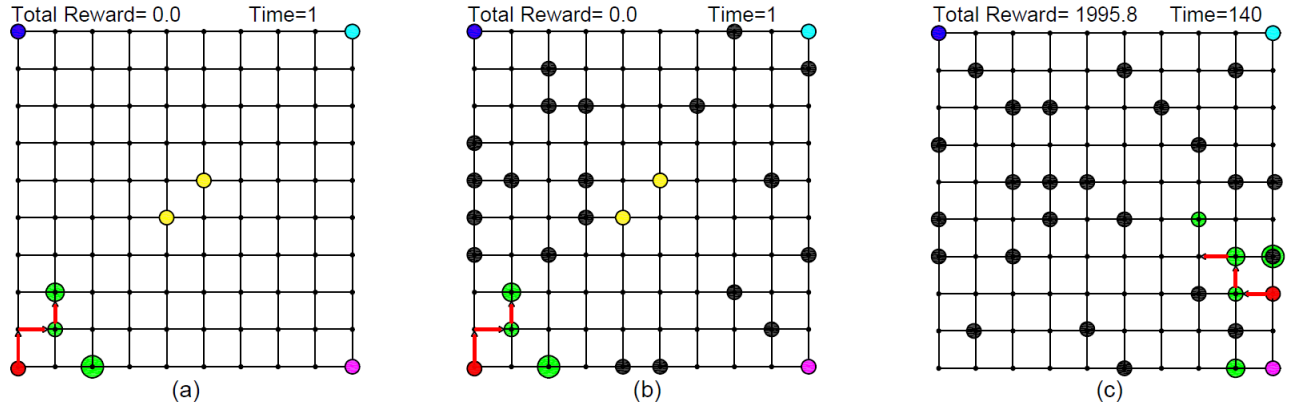


Figure 4: Snapshots of the environment at different time instants. The robot’s position is represented by a red circle, while the randomly generated rewards within the sensing zone of the vehicle are marked by green circles of different sizes proportional to the reward value. The red arrow lines represent the predicted trajectory at the current time. (a) shows the robot’s initial knowledge about the environment at  $t = 1$ s. Initially the robot is only informed of the positions of Base, Supply, Report, and Survey stations, without any *a priori* knowledge of obstacles (i.e., black circles). (b) shows the real setup of the environment scattered with dynamic obstacles at  $t = 1$ s. The environment is assumed to be time-varying with yellow circles (i.e., Survey stations) on and off at different times, which indicates the environment can be infeasible for the robot’s desired task. (c) shows that the environment is infeasible at  $t = 140$ s, where yellow circles are off.

Table I: The comparison of workspace size and computation time.

Workspace size[cell]	$\mathcal{M}$   $Q$	$\mathcal{P}$   $S_{\mathcal{P}}$	Min Time[s]	Max Time[s]	Mean Time[s]	Horizon N
$10 \times 10$	100	2800	0.88	2.91	1.70	4
$10 \times 10$	100	2800	1.12	3.6	1.81	6
$30 \times 30$	900	25200	1.47	5.45	3.12	4
$30 \times 30$	900	25200	1.99	9.12	4.83	8
$50 \times 50$	2500	700000	2.01	14.9	6.11	4

in Fig. 6 indicates that an accepting state has been reached, i.e., the desired task is accomplished for one time. The jumps of energy from  $t = 100$ s to 200s (e.g.,  $t = 100$ s) in Fig. 6 are due to the violation of the desired task whenever the environment becomes infeasible. Nevertheless, the developed control strategy still guarantees the decrease of energy function to satisfy the acceptance condition of  $\mathcal{P}$ . Fig. 7 shows the collected local time-varying reward. The simulation video is provided<sup>3</sup>.

In order to demonstrate scalability and computational complexity of the framework, we repeat the control synthesis introduced above for workspace with different sizes. Specifically, each rectangular state of previous  $10 \times 10$  grid-like graph are further divided into the number of grid-cells  $3^2$ ,  $5^2$ . The dimensions of resulting graph, DTS  $\mathcal{T}$ , and relaxed product automaton  $\mathcal{P}$ , and the maximum, minimum and mean time taken to solve the predicted trajectories at each time-step are shown in Table I, where we also analysis how the various horizon will influence the computations. Due to the off-line computation for largest-self reachable sets that always remains the same, we omit its time comparison.

From table I, we can see that the computational time at each time will be dramatically influenced by updated process

involving recomputing the energy function based on updated knowledge. The benefits of RHC based algorithm in this paper is that the proposed algorithm only need to consider the local scale optimization problem and the energy constraints will ensure the global task satisfaction. As a result, the minimum solving time at each time-step will be slightly influenced.

### B. Experiment results

Experiments were performed on a mobile robot, Khepera IV, to verify the developed control strategy. The workspace is about  $48'' \times 96''$ , consisting of  $4 \times 8$  square cells, as shown in Fig. 8, where the bottom figure shows the experiment workspace while the top figure shows the corresponding simulated workspace. The robot is allowed to transit between adjacent cells, i.e., the robot at a cell has four possible actions, “up,” “down,” “right,” and “left.” Consider three areas of interest,  $P_1$ ,  $P_2$ , and  $P_3$ , which correspond to orange, green, and cyan cells, respectively. The desired task of the robot is to avoid obstacles (i.e., carbon boxes in Fig. 8) and visit  $P_1$ ,  $P_2$ , and  $P_3$  sequentially and infinitely often, which is expressed as an LTL specification

$$\begin{aligned} \phi_s = & \square \diamond P_1 \\ & \wedge \square P_1 \rightarrow \circ (\neg P_1 \cup P_2) \\ & \wedge \square P_2 \rightarrow \circ (\neg P_2 \cup P_3). \end{aligned} \quad (8)$$

The robot is assumed to know the locations of  $P_1$ ,  $P_2$ , and  $P_3$ , without knowing the obstacle positions. It is possible that the preassigned task  $\phi$  cannot be fully accomplished, due to unexpected obstacles. Fig. 8 shows an infeasible case of  $\phi_s$ , where  $P_3$  is surrounded by obstacles and not accessible by the robot. Therefore, the task (8) cannot be fully realized, and the robot has to revise its motion plan and adapts to the real environment. In addition, each cell is assumed to have a time-varying reward, randomly generated from a uniform

<sup>3</sup><https://www.youtube.com/watch?v=RyRnKXDDH5U&t=30s>

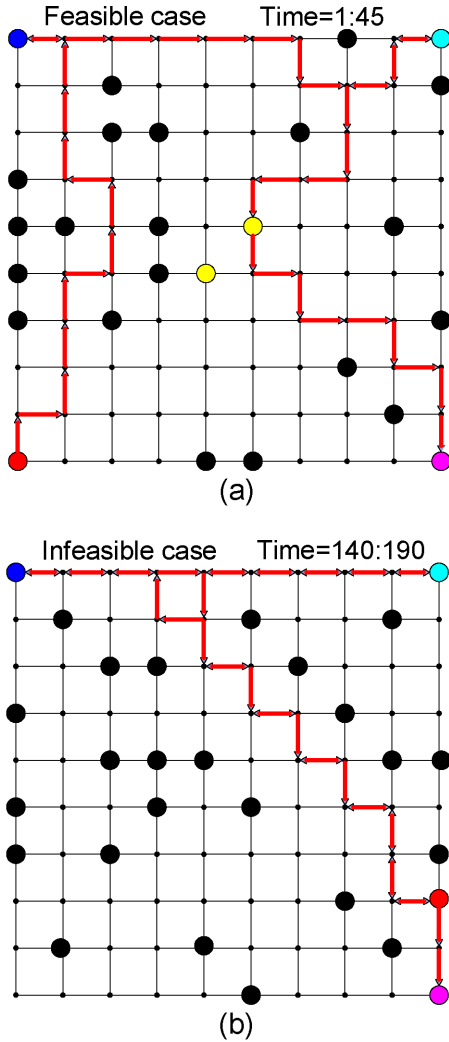


Figure 5: The robot trajectories in feasible and infeasible cases of  $\phi_s$ , respectively. In (a), the environment is fully feasible from  $t = 1s$  to  $t = 45s$ , and the robot successfully completes the desired task (7). In (b), the environment is infeasible from  $t = 140s$  to  $t = 190s$ , where yellow circles do not exist. The robot revises its motion to only sequentially visit Base, Supply, and Report stations. In both (a) and (b), the planned path maximizes the reward collection in a receding horizon manner.

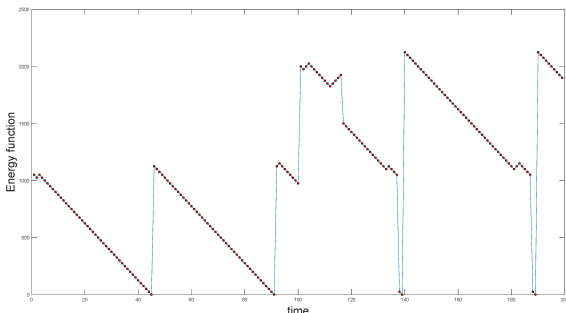


Figure 6: Plot of the energy function during mission operation.

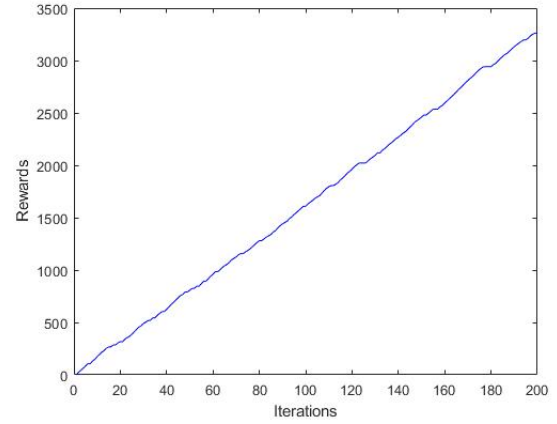


Figure 7: Plot of accumulative collected time-varying rewards.

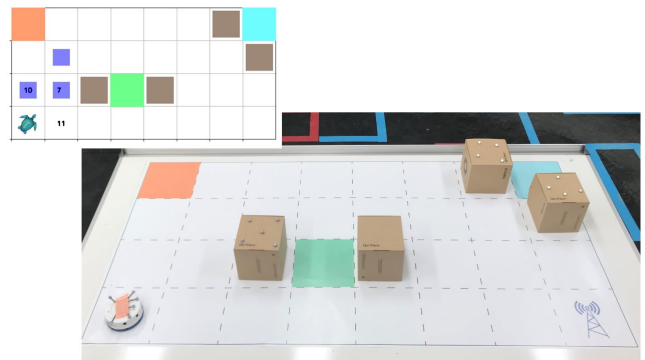


Figure 8: The workspace of the real environment (bottom) and the simulated environment (top). The turtle represents the robot, and the blue squares represent the predicted trajectory, where the number indicates the locally observed rewards.

distribution in the range  $[5, 15]$ . The robot is desired to maximize reward collection while performing the task (8).

The online motion planning strategy in Algorithm 2 was implemented in python on a VMware with a 3.6 GHz Quad-core CPU and 8 GB of RAM. The robot actuation module was implemented on Linux with an Optitrack motion capture system providing real-time position feedback of the robot. The Büchi Automaton  $\mathcal{B}_s$  has  $|S_s| = 12$  states, and the DTS  $\mathcal{T}$  has  $|Q| = 32$ . The relaxed product automaton  $\mathcal{P}$  has  $|S_{\mathcal{P}}| = 384$  states. The horizon in RHC was selected as  $N = 4$ , and the computation of Algorithm 2 at each iteration took 0.25s. During implementation of Algorithm 2, the obstacles can be randomly moved, and the robot usually took about 0.5s to update its motion plan. The experiment video is provided<sup>4</sup>.

## VII. CONCLUSIONS

An RHC-based online motion planning strategy with partially infeasible LTL specifications is developed in this work to enable the autonomous robot to maximize reward collection while considering hard and soft LTL constraints. Motion planning in an uncertain environment can be better modeled

<sup>4</sup><https://youtu.be/16j6TmVUrTk>

by a Markov decision process. Future research will consider extending this work with more realistic robot models and advanced learning based motion planning. Additional research will also consider extending the current work to continuous state space using hybrid control.

### Acknowledgments

We thank Marius Kloetzler, Xuchu Ding, and Calin Belta for their software and open source.

### REFERENCES

- [1] T. Luettel, M. Himmelsbach, and H.-J. Wuensche, "Autonomous ground vehicles-concepts and a path to the future." *Proc. IEEE*, vol. 100, pp. 1831–1839, 2012.
- [2] W. Zhao, Q. Meng, and P. W. Chung, "A heuristic distributed task allocation method for multivehicle multitask problems and its application to search and rescue scenario," *IEEE Trans Cybern.*, vol. 46, no. 4, pp. 902–915, 2016.
- [3] X. Wu, Z. Li, Z. Kan, and H. Gao, "Reference trajectory reshaping optimization and control of robotic exoskeletons for human-robot co-manipulation," *IEEE Trans Cybern.*, 2019.
- [4] C. Ton, Z. Kan, and S. S. Mehta, "Obstacle avoidance control of a human-in-the-loop mobile robot system using harmonic potential fields," *Robotica*, vol. 36, no. 4, pp. 463–483, 2018.
- [5] R. J. Downey, T.-H. Cheng, M. J. Bellman, and W. E. Dixon, "Switched tracking control of the lower limb during asynchronous neuromuscular electrical stimulation: Theory and experiments," *IEEE transactions on cybernetics*, vol. 47, no. 5, pp. 1251–1262, 2016.
- [6] M. Pi, L. Zhijun, Q. Li, Z. Kan, C. Xu, Y. Kang, C.-Y. Su, and C. Yang, "Biologically inspired deadbeat control of robotic leg prostheses," *IEEE/ASME Trans. Mechatronics*, 2020.
- [7] E. Rimon and D. Koditschek, "Exact robot navigation using artificial potential functions," *IEEE Trans. Robot. Autom.*, vol. 8, no. 5, pp. 501–518, Oct 1992.
- [8] A. H. Halim and I. Ismail, "Combinatorial optimization: comparison of heuristic algorithms in travelling salesman problem," *Arch. Comput. Methods Eng.*, vol. 26, no. 2, pp. 367–380, 2019.
- [9] P. Vansteenwegen, W. Souffriau, and D. Van Oudheusden, "The orienteering problem: A survey," *Eur. J. Oper. Res.*, vol. 209, no. 1, pp. 1–10, 2011.
- [10] C. Belta, A. Bicchi, M. Egerstedt, E. Frazzoli, E. Klavins, and G. J. Pappas, "Symbolic planning and control of robot motion," *IEEE Robot. Autom. Mag.*, vol. 14, no. 1, pp. 61–70, 2007.
- [11] S. L. Smith, J. Tumova, C. Belta, and D. Rus, "Optimal path planning for surveillance with temporal-logic constraints," *Int. J. Robotics Res.*, vol. 30, no. 14, pp. 1695–1708, 2011.
- [12] M. Guo and D. V. Dimarogonas, "Multi-agent plan reconfiguration under local LTL specifications," *Int. J. Robotics Res.*, vol. 34, no. 2, pp. 218–235, 2015.
- [13] Y. Kantaros and M. M. Zavlanos, "Distributed intermittent connectivity control of mobile robot networks," *IEEE Trans. Autom. Control*, vol. 62, no. 7, pp. 3109–3121, 2017.
- [14] L. Lindemann, J. Nowak, L. Schönabächler, M. Guo, J. Tumova, and D. V. Dimarogonas, "Coupled multi-robot systems under linear temporal logic and signal temporal logic tasks," *IEEE Trans. Control Syst. Technol.*, 2019.
- [15] M. Cai, H. Peng, Z. Li, and Z. Kan, "Learning-based probabilistic ltl motion planning with environment and motion uncertainties," *IEEE Trans. Autom. Control*, 2020.
- [16] M. Cai, Z. Li, H. Gao, S. Xiao, and Z. Kan, "Optimal probabilistic motion planning with partially infeasible ltl constraints," *arXiv preprint arXiv:2007.14325*, 2020.
- [17] M. Cai, S. Xiao, B. Li, Z. Li, and Z. Kan, "Reinforcement learning based temporal logic control with maximum probabilistic satisfaction," in *Proc. Int. Conf. Robot. Autom.* Xi'an, China: IEEE, 2021, pp. 806–812.
- [18] B. Lacerda, F. Faruq, D. Parker, and N. Hawes, "Probabilistic planning with formal performance guarantees for mobile service robots," *Int. J. Robot. Res.*, vol. 38, no. 9, pp. 1098–1123, 2019.
- [19] I. Cizelj and C. Belta, "Control of noisy differential-drive vehicles from time-bounded temporal logic specifications," *Int. J. Robot. Res.*, vol. 33, no. 8, pp. 1112–1129, 2014.
- [20] P. Schillinger, M. Bürger, and D. V. Dimarogonas, "Simultaneous task allocation and planning for temporal logic goals in heterogeneous multi-robot systems," *Int. J. Robot. Res.*, vol. 37, no. 7, pp. 818–838, 2018.
- [21] A. Jones, M. Schwager, and C. Belta, "Information-guided persistent monitoring under temporal logic constraints," in *Proc. Am. Control Conf. IEEE*, 2015, pp. 1911–1916.
- [22] M. Guo, C. P. Bechlioulis, K. J. Kyriakopoulos, and D. V. Dimarogonas, "Hybrid control of multiagent systems with contingent temporal tasks and prescribed formation constraints," *IEEE Trans. Control Network Syst.*, vol. 4, no. 4, pp. 781–792, 2017.
- [23] T. Wongpiromsarn, U. Topcu, and R. M. Murray, "Receding horizon temporal logic planning," *IEEE Trans. Autom. Control*, vol. 57, no. 11, pp. 2817–2830, 2012.
- [24] X. Ding, M. Lazar, and C. Belta, "LTL receding horizon control for finite deterministic systems," *Automatica*, vol. 50, no. 2, pp. 399–408, 2014.
- [25] Q. Lu and Q.-L. Han, "Mobile robot networks for environmental monitoring: A cooperative receding horizon temporal logic control approach," *IEEE Trans. Cybern.*, vol. 49, no. 2, pp. 698–711, 2018.
- [26] A. Ulusoy and C. Belta, "Receding horizon temporal logic control in dynamic environments," *Int. J. Robotics Res.*, vol. 33, no. 12, pp. 1593–1607, 2014.
- [27] V. Raman, A. Donzé, M. Maasoumy, R. M. Murray, A. Sangiovanni-Vincentelli, and S. A. Seshia, "Model predictive control with signal temporal logic specifications," in *Proc. IEEE Conf. Decis. Control. IEEE*, 2014, pp. 81–87.
- [28] J. Tumova and D. V. Dimarogonas, "A receding horizon approach to multi-agent planning from local ltl specifications," in *Am. Control Conf. IEEE*, 2014, pp. 1775–1780.
- [29] S. S. Farahani, R. Majumdar, V. S. Prabhu, and S. E. Z. Soudjani, "Shrinking horizon model predictive control with chance-constrained signal temporal logic specifications," in *Proc. IEEE Am. Control Conf.*, 2017, pp. 1740–1746.
- [30] C. I. Vasile, X. Li, and C. Belta, "Reactive sampling-based path planning with temporal logic specifications," *The International Journal of Robotics Research*, p. 0278364920918919, 2020.
- [31] J. Tumova, G. C. Hall, S. Karaman, E. Frazzoli, and D. Rus, "Least-violating control strategy synthesis with safety rules," in *Proc. Int. Conf. Hybrid Syst., Comput. Control*, 2013, pp. 1–10.
- [32] L. I. R. Castro, P. Chaudhari, J. Tumova, S. Karaman, E. Frazzoli, and D. Rus, "Incremental sampling-based algorithm for minimum-violation motion planning," in *52nd IEEE Conference on Decision and Control. IEEE*, 2013, pp. 3217–3224.
- [33] M. Lahijanian, S. Almagor, D. Fried, L. E. Kavraki, and M. Y. Vardi, "This time the robot settles for a cost: A quantitative approach to temporal logic planning with partial satisfaction," in *Twenty-Ninth AAAI Conference on Artificial Intelligence*, 2015.
- [34] M. Lahijanian, M. R. Maly, D. Fried, L. E. Kavraki, H. Kress-Gazit, and M. Y. Vardi, "Iterative temporal planning in uncertain environments with partial satisfaction guarantees," *IEEE Trans. Robot.*, vol. 32, no. 3, pp. 583–599, 2016.
- [35] H. Rahmani and J. M. O'Kane, "Optimal temporal logic planning with cascading soft constraints," in *2019 IEEE/RSJ International Conference on Intelligent Robots and Systems (IROS)*. IEEE, 2019, pp. 2524–2531.
- [36] K. Kim and G. E. Fainekos, "Approximate solutions for the minimal revision problem of specification automata," in *IEEE Int. Conf. Intell. Robot. and Syst.*, 2012, pp. 265–271.
- [37] K. Kim, G. E. Fainekos, and S. Sankaranarayanan, "On the revision problem of specification automata," in *Proc. IEEE Int. Conf. Robot. Autom.*, 2012, pp. 5171–5176.
- [38] J. Tumova, L. I. R. Castro, S. Karaman, E. Frazzoli, and D. Rus, "Minimum-violation ltl planning with conflicting specifications," in *2013 American Control Conference*. IEEE, 2013, pp. 200–205.
- [39] H. Rahmani and J. M. O'Kane, "What to do when you can't do it all: Temporal logic planning with soft temporal logic constraints," *2020 IEEE/RSJ International Conference on Intelligent Robots and Systems (IROS)*, 2020.
- [40] E. M. Clarke, O. Grumberg, and D. Peled, *Model checking*. MIT press, 1999.
- [41] P. Gastin and D. Oddoux, "Fast LTL to Büchi automata translation," in *Int. Conf. Comput. Aided Verif.* Springer, 2001, pp. 53–65.
- [42] C. Baier and J.-P. Katoen, *Principles of model checking*. MIT press, 2008.
- [43] E. M. Wolff, U. Topcu, and R. M. Murray, "Optimization-based trajectory generation with linear temporal logic specifications," in *IEEE Int. Conf. Robot. Autom.*, 2014, pp. 5319–5325.

- [44] K. Leahy, A. Jones, M. Schwager, and C. Belta, "Distributed information gathering policies under temporal logic constraints," in *Proc. IEEE Conf. Decis. Control.*, 2015, pp. 6803–6808.
- [45] M. Kloetzer and C. Belta, "A fully automated framework for control of linear systems from temporal logic specifications," *IEEE Trans. Autom. Control*, vol. 53, no. 1, pp. 287–297, 2008.
- [46] M. Cai, H. Peng, Z. Li, H. Gao, and Z. Kan, "Receding horizon control based motion planning with partially infeasible ltl constrains," *IEEE Control Systems Letters*, 2020.
- [47] T. Babiak, M. Křetínský, V. Řehák, and J. Strejček, "Ltl to Büchi automata translation: Fast and more deterministic," in *Int. Conf. Tools Alg. Const. Anal. Syst.* Springer, 2012, pp. 95–109.